Molecular Dynamics of a 15-Residue Poly(L-alanine) in Water: Helix Formation and Energetics

Mitsunori Takano,* Takahisa Yamato,† Junichi Higo,‡ Akira Suyama, and Kuniaki Nagayama§

Contribution from the Department of Life Sciences, Graduate School of Arts and Sciences, University of Tokyo, 3-8-1, Komaba, Meguro-ku, Tokyo 153-8902, Japan, Department of Physics, Graduate School of Science, Nagoya University, Furo-cho, Chikusa-ku, Nagoya 464-8602, Japan, Biomolecular Engineering Research Institute, 6-2-3, Furuedai, Suita, Osaka 565-0874, Japan, and National Institute for Physiological Sciences, Myodaiji, Okazaki 444-8585, Japan

Received August 13, 1998

Abstract: We present a molecular dynamics study of the α-helix formation in a system consisting of a 15-residue poly(L-alanine) and surrounding water molecules. By applying a relatively high temperature, we observed the α-helix formation several times during a 17-ns run, and reversible helix−coil transitions were also observed. The α-helix formations were usually initiated by the β-turn structures. A crank-shaft-like motion of the peptide was included in the folding process. In the formed α-helical domains, substantial 3_{10}-helix formations were found especially at the termini, as observed by the NMR study. The folding time scale at room temperature estimated from our simulation was found to lie in the range of 100 ns, which is in accord with the time scale of the T-jump experiments. The total energy of the whole system was lower in the α-helix state than in the random-coil state by 20.4 ± 4.8 kcal/mol, which is consistent with the experimental value obtained by calorimetry. This energy decrease in forming the α-helix was mainly caused by the Coulombic energy and the torsional energy.

Introduction

Recently, the technique of observing the initial process of protein folding has been developed, and the events occurring on a sub-microsecond time scale can be detected by the temperature jump using a nanosecond pulse laser.[1−4] For example, in myoglobin, the formation of α-helices is found to be complete within 1 μs, and the helices then coalesce to form a nativelike structure in the following microseconds.[1−4] The α-helix formation of a short alanine-rich peptide is directly observed with the same technique, and the time scale of the α-helix formation is reported to be about 180 ns.[5,6] In this connection, the β-sheet formation is found to be slower (i.e., several microseconds) than the α-helix formation.[7] These experimental observations of the time course of the secondary-structure formations not only provide a clue to understanding the mechanism of the protein folding,[8−13] but also make it possible to directly compare the two peptide-folding events observed by the experiments and by the computer simulations with atomic resolution.

The atomic-resolution computer simulations of large molecules, however, require considerable computer power, and the simulation time-range is restricted to around 10 ns, except for a few very recent studies.[14,15] With this limitation, the folding simulation of even a small-sized protein is not tractable, whereas the folding simulation of a short peptide toward the regular structure such as the α-helix seems to be feasible, since the α-helix formation is rapid. In practice, a number of simulations of short peptides have been performed starting from the α-helical structure immersed in explicit water molecules,[16−23] where the stability of the α-helix was investigated. In most cases, only an irreversible unfolding process was observed. The folding simulation, however, is difficult, because the peptide chain is subject to being trapped in metastable states and it takes a long time to get out of them. If water molecules are not explicitly treated to reduce the degrees of freedom to be simulated, it is possible to perform simulations long enough to observe the

* To whom correspondence should be addressed. E-mail: takano@santa.c.u-tokyo.ac.jp.

† Nagoya University.

‡ Biomolecular Engineering Research Institute.

§ National Institute for Physiological Sciences.

(1) Ballew, R. M.; Sabelko, J.; Gruebele, M. *Proc. Natl. Acad. Sci. U.S.A.* **1996**, *93*, 5759−5764.

(2) Gilmanshin, R.; Williams, S.; Callender, R. H.; Woodruff, W. H.; Dyer, R. B. *Proc. Natl. Acad. Sci. U.S.A.* **1997**, *94*, 3709−3713.

(3) Gilmanshin, R.; Williams, S.; Callender, R. H.; Woodruff, W. H.; Dyer, R. B. *Biochemistry* **1997**, *36*, 15006−15012.

(4) Gilmanshin, R.; Callender, R. H.; Dyer, R. B. *Nat. Struct. Biol.* **1998**, 5, 363−365.

(5) Williams, S.; Causgrove, T. P.; Gilmanshin, R.; Fang, K. S.; Callender, R. H.; Woodruff, W. H.; Dyer, R. B. *Biochemistry* **1996**, *35*, 691−697.

(6) Thompson, P. A.; Eaton, W. A.; Hofrichter, J. *Biochemistry* **1997**, *36*, 9200−9210.

(7) Muñoz, V.; Thompson, P. A.; Hofrichter, J.; Eaton, W. A. *Nature* **1997**, *390*, 196−199.

(8) Bryngelson, J. D.; Onuchic, J. N.; Socci, N. D.; Wolynes, P. G. *Proteins* **1995**, *21*, 167−195.

(9) Fersht, A. R. *Proc. Natl. Acad. Sci. U.S.A.* **1995**, *92*, 10869−10873.

(10) Guo, Z.; Brooks, C. L., III; Boczko, E. M. *Proc. Natl. Acad. Sci. U.S.A.* **1997**, *94*, 10161−10166.

(11) Lazaridis, T.; Karplus, M. *Science* **1997**, *278*, 1928−1931.

(12) Karplus, M. *Folding Des.* **1997**, *2*, S69−S75.

(13) Dill, K. A.; Chan, H. S. *Nat. Struct. Biol.* **1997**, *4*, 10−19.

(14) Duan, Y.; Wang, L.; Kollman, P. A. *Proc. Natl. Acad. Sci. U.S.A.* **1998**, *95*, 9897−9902. Duan, Y.; Kollman, P. A. *Science* **1998**, *282*, 740−744.

(15) Daura, X.; Jaun, B.; Seebach, D.; van Gunsteren, W. F.; Mark, A. E. *J. Mol. Biol.* **1998**, *280*, 925−932.

10.1021/ja982919c CCC: $18.00
Published on Web 01/14/1999

folding events of the α-helix.[24−27] Actually, we have observed a number of helix−coil transitions of a polyalanine chain by using the Nosé−Hoover heat bath.[27]

By using a short peptide that contains four or five amino acids, the reverse turn formations have been simulated in explicit water.[28,29] Tobias et al. showed a 2.2-ns molecular dynamics simulation of reverse turn formations with a penta-peptide,[28] and Bashford et al. performed a longer simulation with a tetra-peptide for 7.7 ns and observed enough transitions to conduct a thermodynamic analysis.[29] These simulations shed light on the mechanism of nucleus formation of an α-helix. However, there has not been a simulation of an α-helix formation using a longer peptide in explicit water, starting from the structure other than the α-helical one. Although the simulation with explicit water is more time-consuming than that with an approximated solvation method such as a continuum model, it is advantageous to obtain a more realistic picture of nature, because approximations made there are kept to a minimum without losing the many body interactions between the solute and the solvents.

In this paper, we report the molecular dynamics (MD) simulations of a 15-residue polyalanine solvated by explicit water molecules. Alanine is thought to be one of the residues that have a high helix propensity.[30−34] The synthesized alanine-rich peptides that contain about 20 residues are found to form α-helical structures in an aqueous environment at room temperature.[35] The native state of the polyalanine, as well as the alanine-rich peptide, would be the α-helical structure at room temperature. Even though the α-helical state may be thermodynamically stable, a difficult problem remains concerning whether the peptide can reach its native state within a limited simulation time. This difficulty can be overcome either by using a simulated annealing procedure or by simulating at a relatively high temperature. Actually we were able to observe the α-helix formation several times during a 17-ns simulation, in which reversible helix-coil transitions were involved. We then addressed the following issues from three different viewpoints (i.e., structural, dynamical, and energetic viewpoints). What sort of conformational change is involved in the α-helix formation and disruption? On what time scale does the polyalanine fold into the α-helix? What type of energy (e.g., Coulombic or van der Waals) drives the polyalanine into the α-helix state?

Computational Methods

The system we simulated consisted of a 15-residue polyalanine chain and the surrounding water molecules. The all-atom force field of Weiner et al.[36] was used for the polyalanine chain, of which the N terminus and the C terminus were acetylated and methyl-amidated, respectively. The SPC water[37] was used as the water model, and 2094 water molecules were implemented. A spherical boundary condition was employed with a half-harmonic potential (the force constant was set at 150 kcal/mol/Å^2) to prevent the evaporation of water molecules. This half-harmonic potential took effect only for the water molecules outside the 27.5-Å radius sphere. Inside the sphere, the water molecules contracted to some degree because of the surface tension, resulting in a deformable droplet. The density of water, however, was almost uniform along the radius and nearly equal to the experimentally determined bulk water density at a given temperature,[38] except for the outermost shell region with the radius greater than 23 Å. Since we attempted to simulate such a large conformational change as the helix−coil transition of a polypeptide, we must prepare a sphere large enough to solvate the polypeptide of any conformation. This requirement was fulfilled because the effective radius (or radius of gyration) of the peptide, which usually lay between 7 and 11 Å during the simulation period, was sufficiently smaller than the 27.5-Å radius. In addition, the end-to-end distance of the fully extended conformation was about 55 Å, which is equal to the diameter of the sphere we used. To keep the peptide close to the center against the translational motion (diffusion), the gravity center of the peptide was anchored to the origin of the sphere with a harmonic potential (the force constant was set at 15 kcal/mol/Å^2), while the peptide was free to rotate. We chose an artificially folded left-handed α-helix as the initial structure of the peptide; the left-handed α-helix is thermodynamically less stable than the native *right*-handed α-helix.[39,40] Water molecules were randomly set around the peptide. Since we conducted a long-time simulation during which reversible helix−coil transitions were observed, the choice of the initial structure did not affect the results presented in this paper. We first performed a 2000-step energy minimization. We then carried out 10-ps MD with the initial velocities randomly assigned to realize the Boltzmann distribution at 200 K, and the temperature was raised from 200 to 450 K during this period. After that, we conducted a simulation consisting of a total of 17 ns. This simulation can be divided into three periods: the first period (0−2.5 ns) was an annealing period where the temperature was gradually decreased from 450 to 300 K, the second period (2.5−5 ns) was an equilibrium period where the temperature was raised again and maintained at 450 K, and the last period (5−11 ns) consisted of two independent equilibrium simulations at 450 and 400 K which branched from the point at 5 ns. The equations of motion were numerically integrated using the leapfrog method.[41] The SHAKE algorithm[42] was applied to fix the bond lengths including hydrogen atoms, which allowed us to use the numerical integration time step of 2 fs. The temperature was controlled by weakly coupling with a heat bath.[43] All interactions, including the Coulombic interactions, were calculated without cutoff. Therefore, our system conserves the total energy if the thermostat is not applied. The MD program, PRESTO-v2,[44] was used with modifications to carry out calculations on a special-purpose computer for MD simulations.[45,46] The MD trajectory was saved every 500 steps (1-ps interval) for subsequent analysis, where the trajectory points were averaged for every 10 ps duration in order to reduce fluctuations.

Results

α-Helix Formation and Helix−Coil Transition (0−5 ns). During the entire 17-ns simulation, we were able to observe

(16) Tirado-Rives, J.; Jorgensen, W. L. *Biochemistry* **1991**, *30*, 3864−3871.
(17) Soman, K. V.; Karime, A.; Case, D. A. *Biopolymers* **1991**, *31*, 1351−1361.
(18) DiCapua, F. M.; Swaminathan, S.; Beveridge, D. L. *J. Am. Chem. Soc.* **1991**, *113*, 6145−6155.
(19) Daggett, V.; Levitt, M. *J. Mol. Biol.* **1992**, *223*, 1121−1138.
(20) De Loof, H.; Nilsson, L.; Rigler, R. *J. Am. Chem. Soc.* **1992**, *114*, 4028−4035.
(21) van Buuren, A. R.; Berendsen, H. J. C. *Biopolymers* **1993**, *33*, 1159−1166.
(22) Kovacs, H.; Mark, A. E.; Johansson, J.; van Gunsteren, W. F. *J. Mol. Biol.* **1995**, *247*, 808−822.
(23) Hirst, J. D.; Brooks, C. L., III *Biochemistry* **1995**, *34*, 7614−7621.
(24) Okamoto, Y.; Hansmann, U. H. E. *J. Phys. Chem.* **1995**, *99*, 11276−11287.
(25) Sung, S. S.; Wu, X. W. *Proteins* **1996**, *25*, 202−214.
(26) Klein, C. T.; Mayer, B.; Kohler, G.; Wolshann, P. *J. Mol. Struct.* (*THEOCHEM*) **1996**, *370*, 33−34.
(27) Takano, M.; Takahashi, T.; Nagayama, K. *Phys. Rev. Lett.* **1998**, 80, 5691−5694.
(28) Tobias, D. J.; Merts, J. E.; Brooks, C. L., III. *Biochemistry* **1991**, *30*, 6054−6058.
(29) Bashford, D.; Case, D. A.; Choi, C.; Gippert, G. P. *J. Am. Chem. Soc.* **1997**, *119*, 4964−4971.
(30) O′Neil, K. T.; DeGrado, W. F. *Science* **1990**, *250*, 646−651.
(31) Lyu, P. C.; Liff, M. I.; Marky, L. A.; Kallenbach, N. R. *Science* **1990**, *250*, 669−673.
(32) Chakrabartty, A.; Kortemme, T.; Baldwin, R. L. *Protein Sci.* **1994**, *3*, 843−852.
(33) Padmanabhan, S.; York, E. J.; Gera, J.; Stewart, J. M.; Baldwin, R. L. *Biochemistry* **1994**, *33*, 8604−8609.
(34) Okamoto, Y. *Proteins* **1994**, *19*, 14−23.
(35) Marqusee, S.; Robbins, V. H.; Baldwin, R. L. *Proc. Natl. Acad. Sci. U.S.A.* **1989**, *86*, 5286−5290.

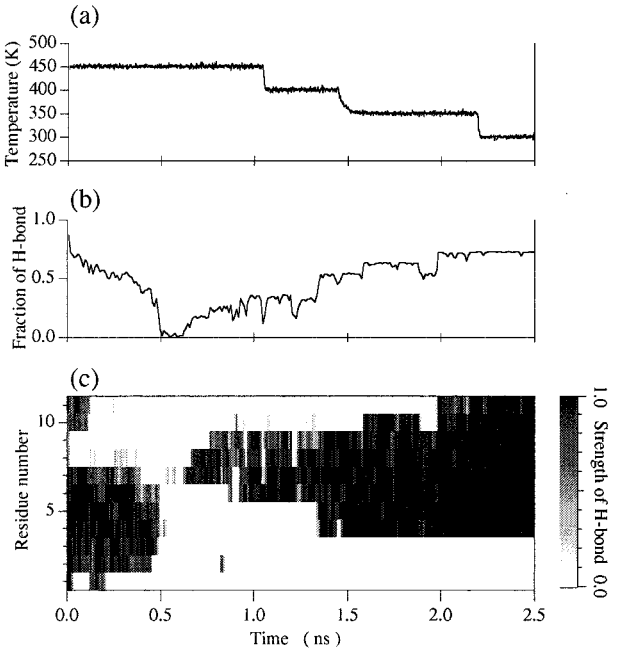

Figure 1. Simulation of the annealing period (0−2.5 ns). Temperature of the system was successively lowered as shown in (a). (b) Trajectory of the fraction of the $i - (i + 4)$ type H-bond in the polyalanine chain. We judged that an H-bond was formed when the distance between the oxygen and the hydrogen was less than 3 Å and the angle of the O−H−N was greater than 120°. The H-bonds within the first 0.5 ns are those of the left-handed α-helix. (c) Spatio-temporal evolution of the $i - (i + 4)$ type H-bonds. The darkness of the shading (gray scale) is in proportion to the H-bond strength, as shown at the right window, which is defined as the ratio of the total H-bonding duration to every 10-ps interval. Note that the residue number, *i*, denotes the *i*th residue with the acceptor oxygen.

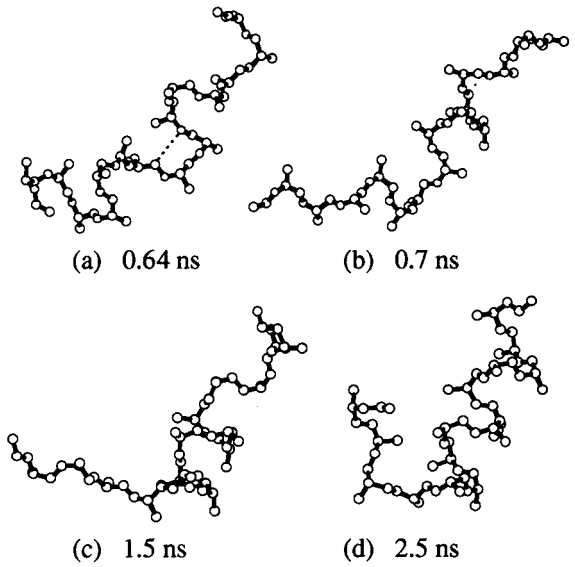

Figure 2. Snapshots of the folding structural change during the annealing period. Main-chain atoms and C_β atoms are displayed. Each structure is superimposed on the structure at 2.5 ns, (d). The N terminus is located at the lower left of each snapshot. The dotted line in (a) shows the initiation H-bond for the right-handed α-helix.

several folding/unfolding events. First, we took a look at the first period (0−2.5 ns), that is, the annealing period at decreasing temperature from 450 to 300 K (Figure 1a). To show the degree of the α-helix formation, we monitored the hydrogen-bond (H-bond) formation between the carboxyl oxygen of residue *i* and amide the hydrogen of residue $i + 4$. The trajectory of the fractional H-bond, which is relative to 11 native H-bonds possible for this peptide, and the spatio-temporal evolution of the H-bond are shown in Figure 1b and c. The initial structure of the peptide was the artificially folded *left*-handed α-helix. In the preparation period, two H-bonds of the left-handed α-helix were immediately broken. For the first 1.05 ns, before cooling, the following events occurred. The small left-handed helical domain on the C-terminal side quickly disappeared, and the disruption of the larger left-handed helical domain followed. (The left-handed α-helix was not observed in the subsequent simulation.) Then, the nascent *right*-handed α-helix appeared at the center of the chain (see Figure 2a). Despite the high temperature, it grew (Figure 2b), and a helical domain with four native H-bonds was formed before 1.05 ns, even though it was fragile. We then cooled the system in a successive manner. The chain further grew first by simultaneously adding two H-bonds on the N-terminal side (Figure 2c) and second, by adding two H-bonds on the C-terminal side. After that, although we further decreased the temperature to 300 K, we could not see any growth; the peptide remained in an almost unchanged conformation, that is, the stable long α-helix ranging from residue 4 to residue 15 with eight native H-bonds and the bent N terminus (Figure 2d).

We next stepped forward to the second period of the equilibrium simulation at 450 K (2.5−5.0 ns). Since the formation of a right-handed α-helix, though fragile, occurred at 450 K in the previous period even before cooling, we attempted to simulate at the constant temperature of 450 K to observe the folding and unfolding (i.e., helix−coil transition), which allowed us to conduct an energetic analysis. In Figure 3, the time evolution of the α-helical H-bond is shown. As we expected, the H-bonds in the α-helical domain immediately became fragile, compared to that at 300 K, and began to fray. However, the growth of the α-helix at the N terminus occurred at ∼3.0 ns (Figure 4a), which was not achieved at 300 K. This elongated α-helix, however, was only temporary. Four native H-bonds at the N terminus disappeared soon, followed by the disruption of the five C-terminal H-bonds. After the disruption of all of the native H-bonds, the chain was in a random coil-like state (Figure 4b). In the random coil-like period, nuclei of the α-helix occasionally appeared but soon disappeared. Among them, the two nuclei that were formed around 3.85 ns (Figure 4c) succeeded in growing (Figure 4d). Then the long α-helix was formed at 4.12 ns (Figure 4e). This refolded α-helix, however, was not stable enough to live long, and turned again into the random coil-like state.

(36) Weiner, S. J.; Kollman, P. A.; Nguyen, D. T.; Case, D. A. *J. Comput. Chem.* **1986**, *7*, 230−252.
(37) Berendsen, H. J. C.; Postma, J. P. M.; van Gunsteren, W. F.; Hermans, J. In *Intermolecular Forces*; Pullman, B., Ed.; Reidel: Dordrecht, 1981; pp 331−342.
(38) Haar, L.; Gallagher, J. S.; Kell, G. S. *NBS/NRC Steam Tables*; Hemisphere Publication Corp.: Washington DC, 1984.
(39) Ripoll, D. R.; Scheraga, H. A. *Biopolymers* **1988**, *27*, 1283−1303.
(40) Sung, S. S. *Biophys. J.* **1995**, *68*, 826−834.
(41) Hockney, R. W. *Methods Comput. Phys.* **1970**, *9*, 135−211.
(42) Ryckaert, J. P.; Ciccotti, G.; Berendsen, H. J. C. *J. Comput. Phys.* **1977**, *23*, 327−341.
(43) Berendsen, H. J. C.; Postma, J. P. M.; van Gunsteren, W. F.; Di Nicola, A.; Haak, J. R. *J. Chem. Phys.* **1984**, *81*, 3684−3690.
(44) Morikami, K.; Nakai, T.; Kidera, A.; Saito, M.; Nakamura, H. *Comput. Chem.* **1992**, *16*, 243−248.
(45) Higo, J.; Endo, S.; Nagayama, K.; Ito, T.; Fukushige, T.; Ebisuzaki, T.; Sugimoto, D.; Miyagawa, H.; Kitamura, K.; Makino, J. *J. Comput. Chem.* **1994**, *15*, 1372−1376.
(46) Komeiji, Y.; Uebayasi, M.; Takata, R.; Shimizu, A.; Itsukashi, K.; Taiji, M. *J. Comput. Chem.* **1997**, *18*, 1546−1563.

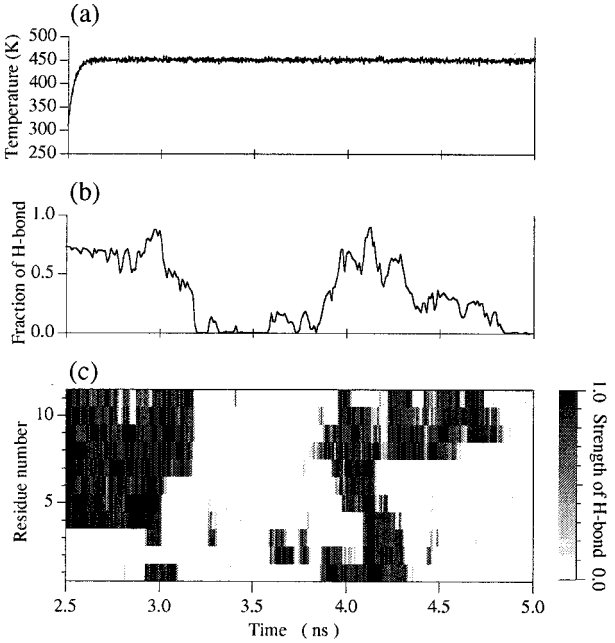

Figure 3. Simulation of the equilibrium period (2.5−5.0 ns). (a) Temperature of the system was raised from 300 K and maintained at 450 K. (b) Trajectory of the fraction of the $i-(i+4)$ type H-bond in the chain. (c) Spatio-temporal evolution of the $i-(i+4)$ type H-bonds. The judgment of the H-bond formation and the definition of the gray scale are identical with those in Figure 1.

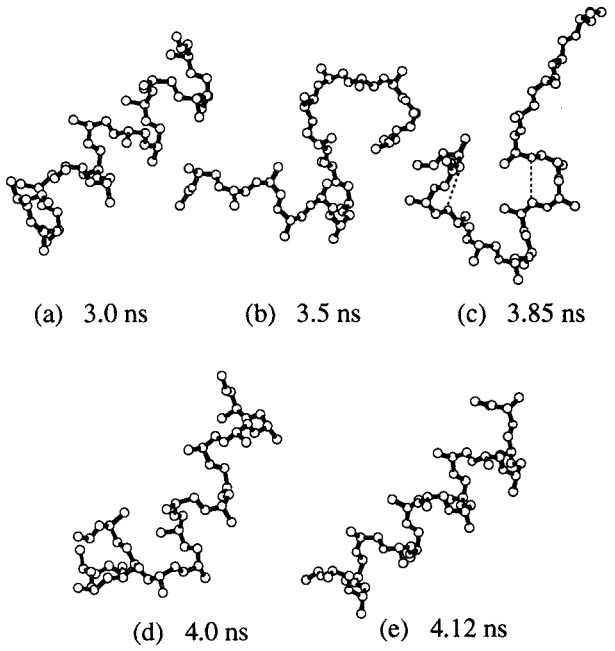

Figure 4. Snapshots of the unfolding/refolding structural change during the equilibrium period at 450 K. In the same way as in Figure 2, only main-chain atoms and C_β atoms are displayed, and each structure is superimposed on the structure at 2.5 ns. The dotted lines in (c) show two independent nucleation H-bonds for the right-handed α-helix.

Other Types of Intrapeptide H-bonds. We now examined the H-bond formations other than the α-helical type, that is, H-bonds between the carboxyl oxygen of residue *i* and the amide hydrogen of residues $i+2$, $i+3$, and $i+5$, which correspond to the γ-turn, the β-turn (or 3_{10}-helix), and the π-helix, respectively. We observed the spatio-temporal evolutions of such H-bonds throughout the above-mentioned two periods (0−2.5 ns and 2.5−5 ns). The spatio-temporal evolution of the $i-(i+3)$ type H-bond (Figure 5b) has a pattern similar to that of the α-helix type, even though the formation is not frequent. A careful look at Figure 5b reveals that substantial formations of the $i-(i+3)$ type H-bond were observed both at the nucleation sites (see also Figures 2a and 4c) and at the ends of the helical domains (especially on the N-terminal side). In addition, we can find that the initial H-bond of the right-handed helix at ∼0.6 ns (Figure 2a) was the remnant of the *left*-handed helix. On the other hand, the $i-(i+2)$ type H-bonds (Figure 5a) showed an opposite pattern from both the $i-(i+3)$ and the $i-(i+4)$ types, although all of them were fragmented and short-lived. The $i-(i+5)$ type H-bonds were rarely observed at the termini (Figure 5c).

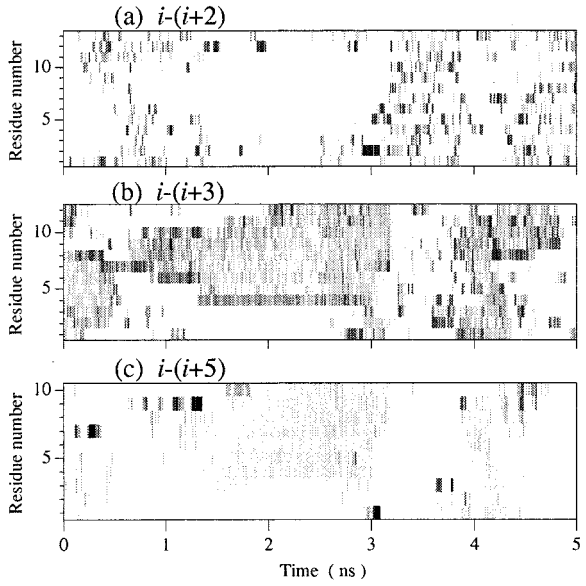

Figure 5. Spatio-temporal evolutions of the H-bond formations other than the $i-(i+4)$ type: (a) the $i-(i+2)$ type H-bond, (b) the $i-(i+3)$ type H-bond, and (c) the $i-(i+5)$ type H-bond. The judgment of the H-bond formation and the definition of the gray scale are identical with those in Figure 1.

Temperature Dependence of α-Helix Formation (5−11 ns). We then proceeded to the third period (5−11 ns). Here, we conducted two independent equilibrium simulations that branched at the point of 5 ns: one was the continuation of the previous equilibrium simulation at 450 K, and the other was another equilibrium simulation where the temperature was lowered and kept at 400 K. The spatio-temporal evolutions of the α-helical H-bonds for both simulations are shown in Figure 6. At 450 K (Figure 6a), after the appearance of short-lived small α-helical domains on the C-terminal side, a long α-helical domain occurred on the N-terminal side, which continued for 2 ns. After this helical domain collapsed, the chain again folded into the α-helix formation from the random coil-like state. On the other hand, at 400 K (Figure 6b), we could not observe any substantial α-helix formation for the first 3 ns. After that, however, we were able to observe the α-helix formation toward the end of this period. Even though the α-helix formation at 400 K was slower than at 450 K, the helical domain, once formed, was more stable at 400 K than at 450 K.

Energetics of α-Helix Formation. We investigated the α-helix formation and disruption from an energetic viewpoint. We focused on the second period (2.5−5 ns), that is, the equilibrium simulation at 450 K, since in this period we could obtain both a long α-helical domain and a disordered random coil. We first looked at the total potential-energy trajectory of the peptide−peptide (P−P) interactions (Figure 7). The potential energy decreased as more native H-bonds were formed. This

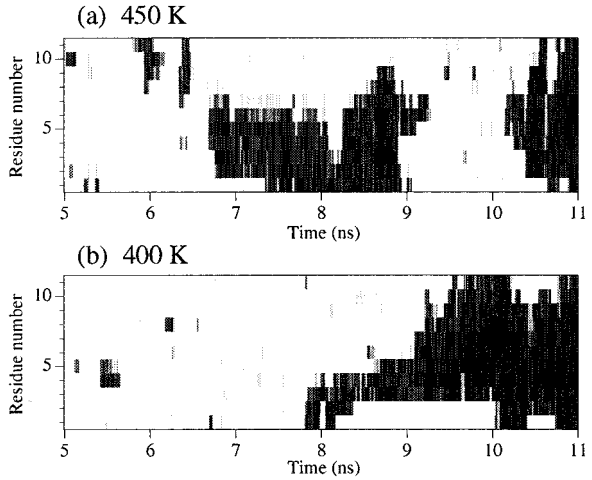

Figure 6. Two independent equilibrium simulations (5.0−11.0 ns) at (a) 450 K, and at (b) 400 K. The spatio-temporal evolutions of the $i-(i+4)$ type H-bonds are shown. The judgment of the H-bond formation and the definition of the gray scale are identical with those in Figure 1.

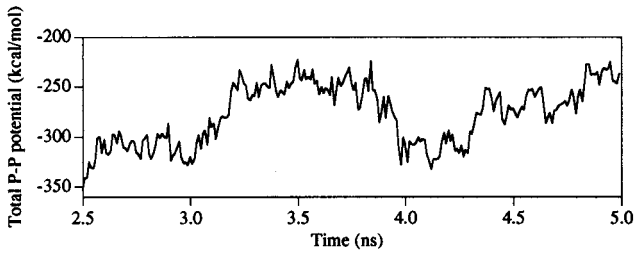

Figure 7. The trajectory of the total potential energy of the peptide-peptide (P−P) interactions during the equilibrium simulation at 450 K (2.5−5.0 ns).

tendency is clearly shown in Figure 8a. We recognized the anticorrelation between the ratio of the native H-bond formed in the polyalanine chain and the total P−P potential energy. Note that the slope of the fitted linear line has an important meaning since it indicates the energy change from the random coil state with no native H-bond to the α-helix state with full native H-bonds. The total P−P potential energy was lower in the α-helix state than in the random coil state by 103.4 ± 2.2 kcal/mol. We then made the same analysis for each ingredient of the total P−P potential energy. The total P−P potential energy is composed of three energies: Coulombic, van der Waals, and geometric (bonding, angular, and torsional) energies. Each of them also had a negative correlation with the native H-bond ratio [Figures 8b−d (note that the vertical axes have varying scales)]. The energy difference between the two states for each energy is summarized in Table 1. We determined that the Coulombic energy had the most significant contribution to the total P−P potential energy.

In contrast to the P−P potential energies, the peptide−water (P−W) potential energies had a positive linear dependence on the native H-bond ratios (Figures 9a and 9b). Again, the Coulombic energy had a greater change than the van der Waals energy (see Table 1). In the meantime, parts c and d of Figure 9 show the water−water (W−W) potential energies, which are the last constituents to be considered. Although there was an inherent large fluctuation, we recognized a negative correlation between the Coulombic energy and the native H-bond ratio, whereas we could not detect a discernible trend in the van der Waals energy. The sum of the P−W and the W−W energy changes associated with the α-helix formation may be regarded

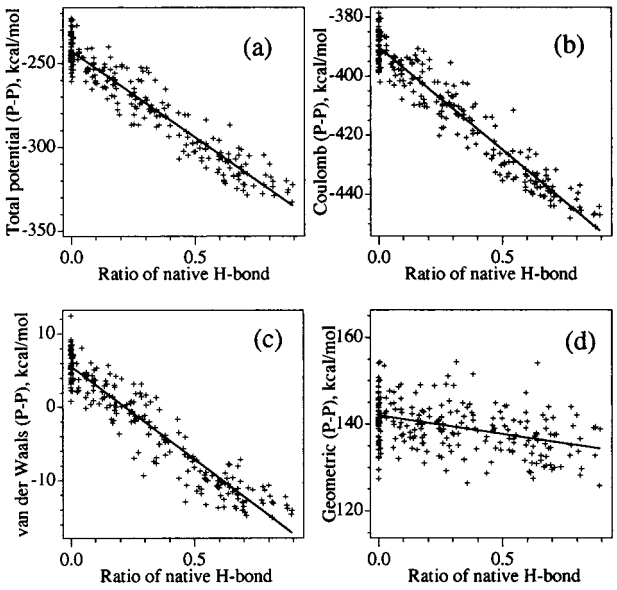

Figure 8. The parametric plots between the peptide−peptide (P−P) potential energies and the ratio of the native [$i-(i+4)$ type] H-bond formed in the polyalanine chain during the equilibrium simulation at 450 K (2.5−5.0 ns): (a) the total potential energy, (b) the Coulombic energy, (c) the van der Waals energy, and (d) the geometric energy. The van der Waals energy contains the 6−12 (Lennerd-Jones) and the 10−12 potential energies, and the geometric energy is composed of the bonding, the angular, and the torsional energies. The data for the first 0.2 ns were discarded to ensure equilibration. The straight lines in the figures represent the least-squares fitted lines as the results of linear regression.

Table 1. Energy Changes from the Coil State to the α-Helix State[a]

	van der Waals	Coulombic	geometric	total
P−P	−25.3 ± 0.6	−69.4 ± 1.4	−8.7 ± 1.3	−103.4 ± 2.2
P−W	21.5 ± 0.8	110.5 ± 2.6		132.0 ± 2.9
W−W	1.2 ± 5.8	−50.2 ± 8.3		−49.0 ± 5.0
system	−2.6 ± 5.8	−9.1 ± 8.1	−8.7 ± 1.3	−20.4 ± 4.8
experiment[b]				−13 to −19

[a] Each entry was obtained from the slope and its standard deviation of the best-fitted line[47] in the parametric plot between the energy and the native H-bond ratio as shown in Figures 8−10. The abbreviations (P−P, P−W, W−W, and system) stand for the peptide−peptide interaction, the peptide−water, the water−water, and the whole system, respectively. Values are in kcal/mol. [b] The enthalpy change was obtained from the calorimetric experiment of Scholtz et al.[60]

as the solvation potential energy change in forming the α-helix. It was then 83.0 ± 5.3 kcal/mol, favoring the random coil state.

So far we have investigated the decomposed energies. We next integrated them. In Figure 10a, we show the parametric plot between the total potential energy of the whole system and the native H-bond ratio. Even though the points are scattered, we found out that the energy decreases as the formation of native H-bonds develops. The energy change that accompanied the helix−coil transition was −20.4 ± 4.8 kcal/mol, favoring the α-helix state. This energy difference was mainly caused by both the Coulombic energy and the geometric energy, whereas the contribution of the van der Waals energy was smaller (see Table 1). We emphasize that the independent energetic analyses for another equilibrium period at 450 K (5−11 ns) yielded the same results; Figure 10b is the equivalent of Figure 10a, and the energy change obtained from Figure 10b was −21.0 ± 2.9 kcal/mol, which is the same, within the error, as obtained from Figure 10a.

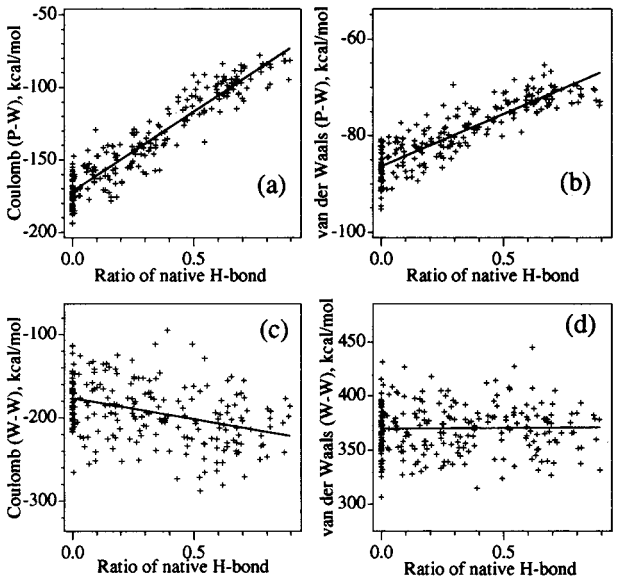

Figure 9. The parametric plots between the intermolecular potential energies and the ratio of the native H-bond formed in the chain during the equilibrium simulation at 450 K (2.7−5.0 ns): (a) the peptide−water (P−W) potential energy for Coulombic, and (b) that for van der Waals; (c) the water−water (W−W) potential energy for Coulombic (arbitrarily shifted upward by 17 800 kcal/mol), and (d) that for van der Waals (arbitrarily shifted downward by 2000 kcal/mol). The straight lines in the figures represent the least-squares fitted lines.

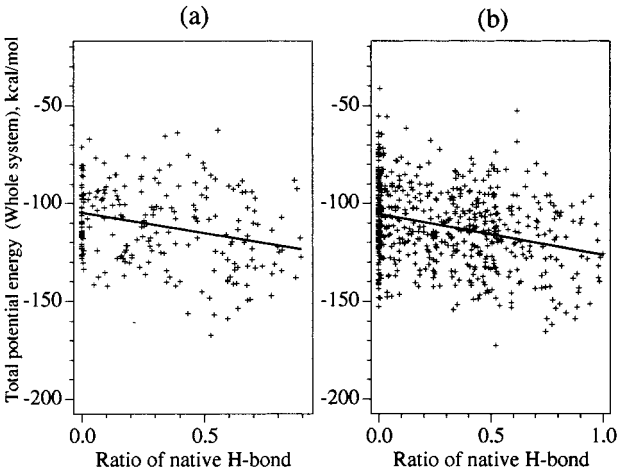

Figure 10. Parametric plot between the total potential energy of the whole system and the ratio of the native H-bond formed in the chain during (a) the equilibrium simulation at 450 K (2.7−5.0 ns) and (b) that for another period (5.0−11.0 ns). The energies are arbitrarily shifted upward by 16000 kcal/mol. The straight lines in the figures represent the least-squares fitted lines.

Discussion

We were able to observe the α-helix formation several times in water. The process in forming (or breaking) native H-bonds has a cooperative nature. Several H-bonds, although not all H-bonds, were cooperatively formed (broken), as was found in the previous MD study of the helix−coil transition without explicit water.[27] Young and Brooks performed the free-energy simulation and determined the difference in cooperativity and stability of the α-helix formation between both ends of a helical domain.[48] Although such a difference was not clear in our simulation presented here, we found that the helical structure on the C terminus is more fragile than that on the N terminus by simulating the α-helix at 400 K (data not shown), which is in accord with the simulation[48] and the experiments.[31,32]

In addition to the α-helical [i.e., $i - (i + 4)$ type] H-bond, we observed the H-bond formations of other types such as the $i - (i + 2)$, the $i - (i + 3)$, and the $i - (i + 5)$ types. The substantial formation of the $i - (i + 3)$ type H-bond at the ends of the α-helical domain is consistent with the NMR study[49] and other theoretical studies.[16,17,48,50] In most cases, the nucleation of the helical structure was initiated by the $i - (i + 3)$ type H-bond formation that belongs to the type I β-turn[51] (see Figure 4c). However, the nucleus found at ∼0.6 ns in the first period (Figure 2a) took the form of the type II β-turn,[51] which was the remnant conformation of the initial left-handed α-helix. It is interesting that the type II β-turn then converted to the type I β-turn by a crankshaft-like counter-rotational motion, which has been thought of as an essential motion of polymers in solution in order to minimize the frictional resistance.[52,53] Regarding the rarely formed $i - (i + 5)$ type H-bond, the formation was merely due to the main-chain H-bonding interaction, not due to the side-chain−side-chain interaction as observed in the simulation of an alanine-rich peptid.[54]

During the equilibrium simulations at 450 K (2.5−11.0 ns), we observed substantial α-helix formation three times. Therefore, the simulated folding time scale at 450 K is supposed to lie in the range of several nanoseconds. This time scale, however, appears to be much faster than the experimentally determined folding time scale of 180 ns. To account for this inconsistency, we made a rough estimation of the folding time scale at room temperature (300 K), assuming the temperature and viscosity dependence of the rate constant according to Kramers' theory in the large viscosity regime.[55,56] Although the α-helix formation involves many reactions, the time scale of adding one H-bond to the existing α-helical segment would provide the lower bounds of the α-helix formation time scale. The barrier height of this process has been extensively studied by free-energy simulations and estimated to be about 2.8 kcal/mol, which is mainly due to the unfavorable steric interactions within the peptide.[48,57] Furthermore, the water viscosity, itself, has a temperature dependence,[58,59] and the value at 450 K is about 6 times smaller than at 300 K; the self-diffusion coefficients of water calculated in our system (data not shown) were in accord with the experimental ones,[58] so that the viscous property of water would be well-simulated. Taking these facts into account, we expected the folding time scale at 300 K to be about 30 times slower than that at 450 K, that is, in the range of 100 ns (see Appendix where the Kramers' rate formula is given together with the comparison between the folding and

(47) Press: W. H.; Teukolsky, S. A.; Vetterling, W. T.; Flannery, B. P. *Numerical Recipes in Fortran*: *The Art of Scientific Computing*, 2nd ed.; Cambridge University Press: New York, 1996; pp 655−660.

(48) Young, W. S.; Brooks, C. L., III. *J. Mol. Biol.* **1996**, *259*, 560−572.

(49) Millhauser, G. L.; Stenland, C. J.; Hanson, P.; Bolin, K. A.; van de Ven, F. J. M. *J. Mol. Biol.* **1997**, *267*, 963−974.

(50) Sheinerman, F. B.; Brooks, C. L., III. *J. Am. Chem. Soc.* **1995**, *117*, 10098−10103.

(51) Rose, G. D.; Gierasch, L. M.; Smith, J. A. *Adv. Protein Chem.* **1985**, *37*, 1−109.

(52) Pear, M. R.; Northrup, S. H.; McCammon, J. A.; Karplus, M.; Levy, R. M. *Biopolymers* **1981**, *20*, 629−632.

(53) Helfand, E. *Science* **1984**, *226*, 647−650.

(54) Shirley, W. A.; Brooks, C. L., III. *Proteins* **1997**, *28*, 59−71.

(55) Kramers, H. A. *Physica* **1940**, *7*, 284−304.

(56) Steinfeld, J. I.; Francisco, J. S.; Hase, W. L. *Chemical Kinetics and Dynamics*; Prentice Hall Inc.: New Jersey, 1989; pp 410−414.

(57) Brooks, C. L., III. *J. Phys. Chem.* **1996**, *100*, 2546−2549.

(58) Krynicki, K.; Green, C. D.; Sawyer, W. *Faraday Discuss. Chem. Soc.* **1978**, *66*, 199−208.

the unfolding rates). This estimated time scale is in agreement with the experimentally determined time scale.[5,6] In addition, the α-helix formation at 400 K is expected to be about 2 times slower than at 450 K, and our results coincide with this prediction of Kramers' theory (see Figure 6).

We found a linear correlation between the ratio of the native H-bonds formed in the polyalanine chain and each of the energies (Figures 8−10). This fact implies that the formation of the native H-bonds played a leading role in our simulation, since it had a crucial effect on the energetics of the whole system including not only that of the polyalanine but also that of the water molecules. The total energy change of the whole system that accompanied the α-helix formation was consistent with the value obtained by the calorimetric experiment of Scholtz et al.[60] (see Table 1). The temperature dependence of the helix−coil energy changes is thought to be small because of the small heat-capacity change as to the helix−coil transition of the polyalanine chain (ca. 0.027 kcal/mol/K).[61,62]

The subsequent question then concerns what sort of energy caused this total energy decrease in forming the α-helix. By dividing the total energy, we determined that the dominant energies that stabilize the α-helix state were the Coulombic and the geometric energies (see the fourth row of Table 1). It has been considered that the main-chain H-bond formation, which is mainly due to the Coulombic interaction, stabilizes the α-helix state,[60,63] although there has been a contradictory opinion.[64,65] Our results support the former opinion. It should be noted, however, that the Coulombic energy decrease associated with the α-helix formation was not simply due to the native H-bond formation in the polypeptide, but was caused by *the sum* of both the intrapeptide (P−P) and the intermolecular (P−W and W−W) H-bonds. The net decrease in the Coulombic energy in folding resulted from the fact that the native intrapeptide H-bond was tighter (or more favorable) than the intermolecular H-bonds. The geometric energy change, another dominant helix-stabilizing factor in our simulation, mainly originated from the torsional energy change. The reason can be explained as follows; in the random coil state, the dihedral angles took various values with high energies, whereas in the α-helix state, they predominantly took the gauche conformer (g^-) which corresponds to an energy minimum.

Finally, it would be interesting to compare our energetic results with that of another group. Braxenthaler et al. simulated an isolated helix fragment of barnase in water starting from the X-ray structure of the native protein,[66] and they observed partially breaking and reforming of main-chain H-bonds. The energy changes that accompanied the breaking or reforming of the main-chain H-bonds are found to be consistent with ours, except for the geometric and especially the torsional energy; the torsional energy was almost unchanged in their simulation in contrast with our previously mentioned result. This is because in their simulation, the peptide did not undergo such a large conformational change as observed in our simulation. At any rate, it is noteworthy that two different MD simulations with different peptides and different force-fields produced a similar result concerning the energy change associated with the main-chain (native) H-bond formation.

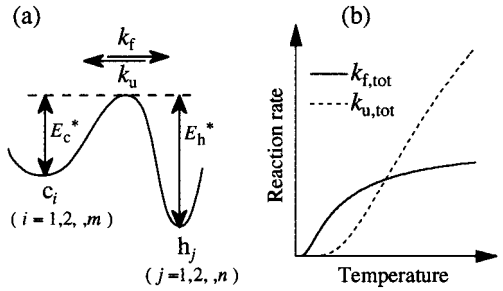

Figure 11. (a) Schematic picture of the helix−coil reactions. (b) General profiles of the total folding and the total unfolding rates ($m/n = 5$, $E_h^*/E_c^* = 5$). See the text for the details.

Conclusion

We demonstrated MD simulations of a 15-residue polyalanine in water, and we observed the α-helix formation several times. The folding events showed a cooperative nature, and it usually began with the $i - (i + 3)$ type H-bond formation. In the folding dynamics of the peptide, a crankshaft-like motion was included, which is thought of as an essential motion of polymer dynamics in solution. The 3_{10}-helix was observed especially at the ends of the α-helical domains. The folding time scale at room temperature estimated from our simulation was about 100 ns, which is in accord with the time scale determined by the T-jump experiments of an alanine-rich peptide. The formation of the native H-bond affected the energies in the system. The peptide−peptide energies and the water−water Coulombic energy had a negative correlation against the ratio of the native H-bond formed in the polyalanine chain, while the peptide−water energies had a positive correlation. The total-energy of the whole system decreased by 20.4 ± 4.8 kcal/mol from the random coil state to the α-helix state, which is consistent with the enthalpy change determined by the calorimetry experiment using an alanine-rich peptide. Our results support the opinion that the main-chain (native) H-bond formation, which is mainly due to the Coulombic interactions, stabilizes the α-helix formation of a short peptide. The torsional energy was also found to contribute as much to the α-helix stability as the Coulombic energy.

Appendix: Kramers' Rate Formula and Comparison between Folding and Unfolding Rates. Kramers' rate for the barrier-crossing reaction (in the large viscosity regime) is described as[55,56]

$$k(T) \propto \gamma(T)^{-1} \exp(-E^*/RT) \qquad (1)$$

where γ, E^*, R, and T are the friction constant, the barrier height, the gas constant, and the temperature, respectively. In Figure 11a, we show the illustration of helix−coil (folding−unfolding) reactions. As already discussed, the rate for the helix formation decreases as temperature decreases. The same is true of the unfolding rate, which was not dealt with in the discussion. Then, we compared the total folding and the total unfolding rates; since each of the coil and the helix states has a number of microstates (c_i's and h_j's in Figure 11a), we considered parallel reactions. To make a general argument, we assumed that the coil and the helix states have m and n microstates, respectively, and that each microstate in the coil (helix) state can reach all of the n (m) ones in the helix (coil) state by overcoming the barrier of

(59) Alberty, R. A. *Physical Chemistry*, 7th ed.; John Wiley: New York, 1987.
(60) Scholtz, J. M.; Marqusee, S.; Baldwin, R. L.; York, E. J.; Stewart, J. M.; Santoro, M.; Bolen, D. W. *Proc. Natl. Acad. Sci. U.S.A.* **1991**, *88*, 2854−2858.
(61) Ooi, T.; Oobatake, M. *J. Biochem.* (*Tokyo*) **1988**, *103*, 114−120.
(62) Ooi, T.; Oobatake, M. *Proc. Natl. Acad. Sci. U.S.A.* **1991**, *88*, 2859−2863.
(63) Avbelj, F.; Fele, L. *J. Mol. Biol.* **1998**, *279*, 665−684.
(64) Yang, A. S.; Honig, B. *J. Mol. Biol.* **1995**, *252*, 351−365.
(65) Wang, L.; O'Connell, T.; Tropsha, A.; Hermans, J. *Biopolymers* **1996**, *39*, 479−489.
(66) Braxenthaler, M.; Avbelj, F.; Moult, J. *J. Mol. Biol.* **1995**, *250*, 239−257.

the same height. The total folding (unfolding) rate, $k_{f,tot}$ ($k_{u,tot}$), then becomes

$$k_{f,tot} = nk_f \propto n \exp(-E_c^*/RT) \quad (2)$$

$$k_{u,tot} = mk_u \propto m \exp(-E_h^*/RT) \quad (3)$$

where k_f and k_u are the rates of a single reaction (see Figure 11a) (we dropped the friction constant because we were concerned with the relative values). By taking the fact that $m > n$ and $E_h^* > E_c^*$ into account, we obtained the general features of $k_{f,tot}$ and $k_{u,tot}$ as shown in Figure 11b; in addition to the decrease of the rates at lower temperature, we noted that there is a specific temperature where the two rates cross. Below that temperature, $k_{f,tot}$ surpasses $k_{u,tot}$ so that the helix state becomes more stable; in fact, a more stable helix was observed at a lower temperature both in our simulation and in the experiments.[5,35] Further calculation of the ratio of the two rates gave us the following expression

$$k_{f,tot}/k_{u,tot} = (n/m) \exp[-(E_c^* - E_h^*)/RT] \quad (4)$$

$$= \exp[-(E_c^* - E_h^*)/RT]\exp[R(\ln n - \ln m)/R] \quad (5)$$

$$= \exp[-(\Delta E - T\Delta S)/RT] \quad (6)$$

where ΔE and ΔS are the energy and the entropy changes from the coil state to the helix state (we used the Boltzmann's relation, $S = R \ln W$, where W is the number of the microstates in each state). Thus, we recognized the correspondence to thermodynamics.

JA982919C